OPEN

Clinical & Translational Immunology (2015) 4, e42; doi:10.1038/cti.2015.18

www.nature.com/cti

ORIGINAL ARTICLE

Immunological evidence and regulatory potential for cell-penetrating antibodies in intravenous immunoglobulin

Aggeliki D Sali[1], Ioannis Karakasiliotis[2], Maria Evangelidou[3], Stratis Avrameas[1] and Peggy Lymberi[1]

Anti-DNA cell-penetrating autoantibodies have been extensively studied in autoimmune but not in normal sera. We investigated herein the presence and properties of cell-penetrating antibodies (CPAbs) in intravenous immunoglobulin (IVIg), a blood product of pooled normal human IgG. IVIg cell penetration was observed into various cell lines, as well as cells from several organs of mice injected intravenously with IVIg therapeutic dose. In all cell types examined *in vitro* and *in vivo*, intracellular IgG localized in the cytoplasm, in contrast to the nuclear accumulation of disease-related CPAbs. IVIg was found to rapidly enter cells via an energy-independent mode. The CPAb-fraction was isolated and found to be polyreactive to nuclear and cytoplasmic components; although it corresponded to ~2% of IVIg, it accounted for its inhibitory effect on splenocyte activation. Investigation of IVIg cell penetration capacity provides insight into its mechanisms of action and may account for some of its beneficial effects in numerous diseases.
Clinical & Translational Immunology (2015) **4,** e42; doi:10.1038/cti.2015.18; published online 2 October 2015

It is well established, mainly from studies conducted up to 2001, that antibodies to nuclear constituents, primarily DNA, commonly detected in the sera from patients with systemic lupus erythematosus or mixed connective tissue disease[1–3] and lupus-prone mice[4,5] are able to penetrate into living cells (cell-penetrating antibodies; CPAbs) and accumulate in the nucleus. CPAbs can enter a wide range of cell types and further induce functional alterations.[3–10] These antibodies exhibit polyreactivity, which appears to confer to their ability to traverse the cell membrane,[11] possibly through interactions with various molecules exposed on the cell surface.[12–17] Their exact mode of entry remains unclear, with contradictory findings supporting mainly an endocytosis-dependent process, but also an energy-independent process.[6,18,19]

These disease-occurring CPAbs share common features (for example, polyreactivity and germ-line gene encoding) with natural antibodies (NAbs) present in healthy individuals.[11,20,21] Despite these similarities, up to date, the existence and the properties of naturally occurring CPAbs have never been directly assessed in normal sera. Some indications only have been provided by the groups of A Borghetti and R Bazin reporting the internalization of intravenous immunoglobulin (IVIg), a therapeutic blood product of pooled normal human IgG, into certain cell types (endothelial, dendritic and B cells).[22–24] IVIg internalization was reported to occur via either an endocytosis-dependent mechanism or spontaneously via an unknown mechanism, followed by modulation of endothelial cell anti-inflammatory response or by alteration of major histocompatibility complex class II antigen presentation, respectively.[24,25] In this study, we focused on unanswered issues concerning the contribution of specific antibody subpopulations in IVIg cell penetration and the subsequent effect(s) on cell function, as well as the biodistribution of IVIg post administration.

RESULTS

IVIg penetrates into various mammalian cell lines

Previous studies showed that antibodies from patients with autoimmune disorders could spontaneously penetrate cells in culture.[1,2,5] To study cell-penetrating capacity of antibodies from healthy individuals, three therapeutic IVIg preparations, from thousands of healthy donors, were used herein as a source of natural IgG antibodies.[26,27] Titration of IVIg in cell penetration assay (0.05–3.2 $mg\,ml^{-1}$ with twofold increments) showed that the optimum concentration was $1.6\,mg\,ml^{-1}$ for all three IVIg, as $3.2\,mg\,ml^{-1}$ gave similar fluorescent intensity, and concentrations lower than 1.6 $mg\,ml^{-1}$ presented a dose-dependent decrease in intensity, resulting in undetectable signal at $0.05\,mg\,ml^{-1}$ (data not shown). Intracellular localization of IVIg was observed using confocal microscopy after incubation of various cell lines with the three different preparations of IVIg at $1.6\,mg\,ml^{-1}$. The same penetration profile in the cytoplasm was observed with all three IVIg preparations and all cell lines tested (Figure 1a; Sandoglobulin-IVIg, representative results). Time-course analysis of this process (at 0, 2, 30, 60, 120 and 240 min) indicated that all three IVIg could be detected intracellularly as early as 2 min post

[1]Department of Immunology, Immunology Laboratory, Hellenic Pasteur Institute, Athens, Greece; [2]Department of Microbiology, Molecular Virology Laboratory, Hellenic Pasteur Institute, Athens, Greece and [3]Department of Immunology, Molecular Genetics Laboratory, Hellenic Pasteur Institute, Athens, Greece
Correspondence: Dr P Lymberi, Department of Immunology, Immunology Laboratory, Hellenic Pasteur Institute, 127 Vasilissis Sofias Avenue, 115 21 Athens, Greece.
E-mail: plymberi@pasteur.gr
Received 26 July 2015; accepted 27 July 2015

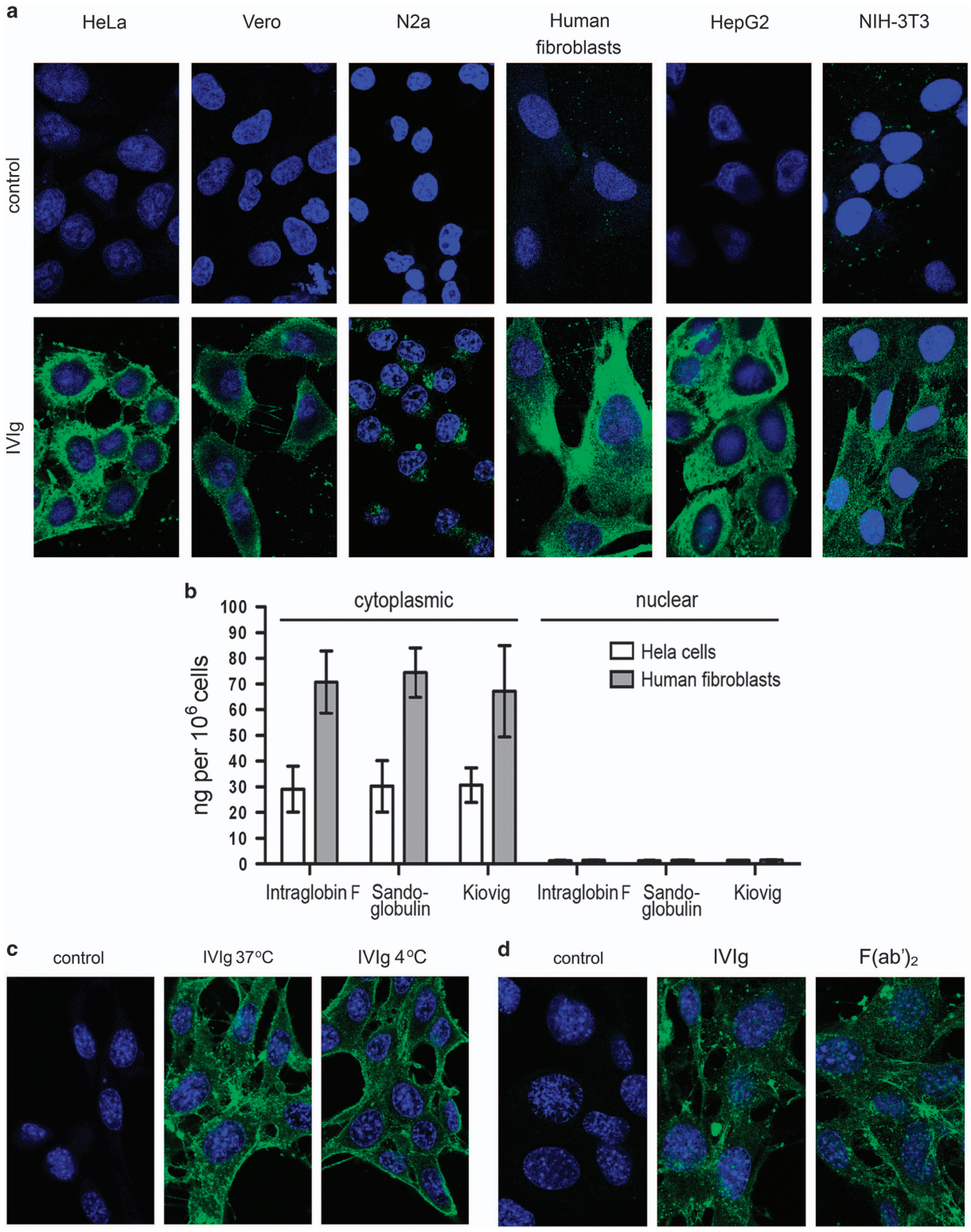

Figure 1 *In vitro* cell penetration of IVIg. Cells were incubated with an IVIg preparation (Sandoglobulin; 1.6 mg ml^{-1}), IVIg-F(ab′)$_2$ fragments (1.6 mg ml^{-1}) or culture medium (control). Confocal sections of IVIg staining (green) after incubation with: (**a**) HeLa, Vero, N2a, Human fibroblasts, HepG2 or NIH-3T3 cells for 2 h at 37 °C. An anti-human IgG (H- and L-chain-specific)-Alexa488 conjugate was used for IVIg detection (green). (**b**) Means ± s.d. of IgG concentrations measured by ELISA in cytoplasmic and nuclear extracts of HeLa cells (white bars) and human fibroblasts (gray bars) obtained after their trypsinization and lysis with hypotonic buffers. Results are obtained from three independent experiments. (**c**) Confocal sections of NIH-3T3 cells after incubation with IVIg for 2 h at 37 °C and 4 °C (pretreated for 30 min at 4 °C) with the use of anti-human IgG (H- and L-chain-specific)-Alexa488 conjugate as detection antibody or (**d**) with IVIg and F(ab')$_2$ detected by anti-human IgG F(ab')$_2$ antibody conjugated to fluorescein isothiocyanate (green). In all cell-imaging assays, TO-PRO-3 iodide (blue) was used for nucleus labeling, and images captured with a x63 HCX PLApo objective lens. Results are representative of at least three independent experiments.

treatment, and the fluorescence intensity plateaued within 2 h (Supplementary Figure 1). To verify that CPAbs occur in individual sera, IgGs from five healthy donors were isolated using protein-G-Sepharose and tested on NIH-3T3 cells under the same conditions. Interestingly, IgGs from all individuals also showed cytoplasmic accumulation (Supplementary Figure 2). Quantitation of intracellular IVIg in HeLa cells and human fibroblasts by ELISA further confirmed the predominant cytoplasmic localization of all IVIg; 35 and 70 ng of IVIg per 10^6 cells, respectively, were measured in the cytoplasmic extracts, whereas undetectable levels were obtained for the nuclear ones (Figure 1b). Notably, cell penetration of IVIg could be achieved even at 4 °C signifying an energy-independent mechanism (Figure 1c). Treatment of cells with cytochalasin D, a known inhibitor of actin polymerization, did not influence Sandoglobulin-IVIg cell penetration (Supplementary Figure 3), suggesting a non-endocytosis mode of entry. Moreover, this entry seems to be $F(ab')_2$-dependent as the enzymic removal of the Fc region did not affect the cytoplasmic localization of IVIg—detected by anti-$F(ab')_2$ secondary antibody—(Figure 1d), without, however, excluding an Fc-assisted uptake. In all cell penetration assays, control cells treated with culture medium presented only background levels of fluorescence.

Identification of antibody fractions of IVIg with cell penetration potential

As heparan sulfate, DNA and histone have been associated with antibody cell penetration,[12–15] we prepared respective immunoadsorbents (IADs) and purified IgG antibody fractions from 100 mg of Intraglobin F-IVIg. The affinity-purified IgG antibodies possessed significantly enhanced reactivity to the autologous antigens compared with the whole IVIg and the effluents derived from each IAD (Figure 2a). The antibodies isolated on histone, heparin and DNA IADs corresponded to 1.2%, 0.48% and 0.45% of whole IVIg, respectively. These antibodies showed a broad range of reactivities against a panel of self and non-self-antigens thus revealing their polyreactive nature (Table 1). Regarding cell penetration, these antibodies were all found to exhibit improved capacity to penetrate NIH-3T3 cells compared with the whole IVIg, as high intracellular fluorescent intensity was obtained at lower concentrations (0.2 mg ml^{-1} of purified antibodies versus 1.6 mg ml^{-1} of whole IVIg; Figure 2b), although IVIg at 0.2 mg ml^{-1} presented far less intracellular fluorescent labeling (data not shown). After exhaustive passages of IVIg through the three different IADs, in a random order as described in Methods, depletion of CPAbs in the effluent was observed. Indeed, analysis by confocal microscopy showed that the penetrating ability of the effluent, tested at the same concentration as IVIg (1.6 mg ml^{-1}), was abrogated (Figure 2b). Semi-quantitative analysis of confocal images from NIH-3T3 cells showed that fluorescent intensity was decreased after depletion of each antibody fraction (ranging from 26 to 35.3%; $P \leqslant 0.01$ for effluents of histone and DNA IADs and $P \leqslant 0.001$ for effluent of heparine IAD), and dramatically decreased when all three fractions were removed (93.9%; $P \leqslant 0.001$; Supplementary Figure 4). Thus, the ability of IVIg to penetrate cells resides within the ~2% of antibodies present in the IVIg preparation.

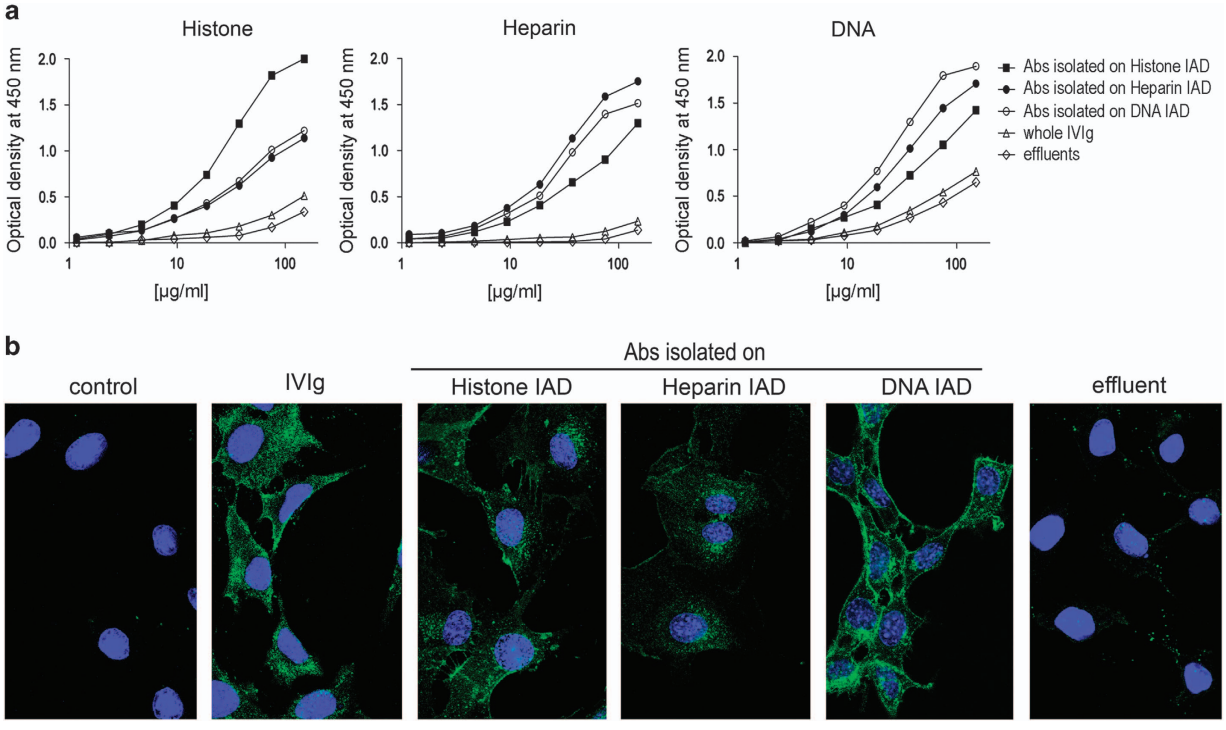

Figure 2 Antibody reactivity and *in vitro* cell penetration capability of IVIg affinity-purified fractions. Affinity-purified specific antibody fractions were isolated from IVIg (Intraglobin F) on histone (■), heparin (●) or DNA (○) immunoadsorbents (IADs) and examined in comparison to the whole IVIg (Δ) or respective IVIg-effluents (◊). (**a**) Reactivity of antibodies (150–1.2 µg ml^{-1}) against histone, heparin and DNA by ELISA, using anti-human IgG-horseradish peroxidase conjugate as secondary antibody. (**b**) Confocal sections of NIH-3T3 cells after incubation for 2 h at 37 °C with the three affinity-purified antibody fractions (0.2 mg ml^{-1}), whole IVIg (1.6 mg ml^{-1}), effluent (1.6 mg ml^{-1}) or culture medium (control). This effluent results from the exhaustive and successive passages of IVIg through all three IADs. IVIg staining (green) revealed with anti-human IgG (H- and L-chain-specific)-Alexa488 and TO-PRO-3 iodide nucleus labeling (blue) observed using a x63 HCX PLApo objective lens. All results are representative of three independent experiments.

Table 1 Reactivities of affinity-purified antibody fractions from Intraglobin F-IVIg, against a panel of antigens

Preparation	*Recovered*[a]	*Antibody reactivity*[b]								
	(%)	*Heparin*	*Histone*	*DNA*	*Actin*	*Tubulin*	*F(ab')$_2$*	*Carbonic anhydrase*	*TNP–BSA*	*Thyroglobulin*
IVIg	—	0.06	0.18	0.35	0.18	0.06	0.06	0.17	0.40	0.29
Abs isolated on histone IAD	1.20	0.65	1.31	0.72	1.02	0.86	0.72	0.93	0.43	0.33
Abs isolated on heparin IAD	0.48	1.13	0.62	1.01	0.68	0.82	0.59	0.81	0.35	0.35
Abs isolated on DNA IAD	0.45	0.98	0.67	1.30	0.65	0.58	0.70	0.71	0.30	0.36

Abbreviations: Abs, antibodies; IAD, immunoadsorbent; IVIg, intravenous immunoglobulin; TNP–BSA, trinitrophenyl–bovine serum albumin.
[a]The amount of isolated IgG recovered from 100 mg (expressed in %) of the IVIg preparation after 3–4 successive passages on the same IAD.
[b]Antibody reactivity against a panel of antigens assessed by ELISA, using anti-human IgG (H- and L-chain-specific)-horseradish peroxidase conjugate, or anti-human IgG (γ-chain-specific)-alkaline phosphatase conjugate in the case of IgG F(ab')$_2$ fragments. Reactivity of samples is expressed as the optical density (at 450 or 405 nm) obtained at an optimum IgG concentration of 37.5 μg ml^{-1}. Representative data from three independent experiments.

Control cells treated with culture medium presented only background levels of fluorescence.

The penetrating fraction of IVIg inhibits the upregulation of CD25 on CD4$^+$ splenocytes

It has been previously reported that IVIg treatment attenuated lymphocyte activation.[24] To investigate whether penetration of IVIg in splenocytes affected their activation status, the expression of the activation marker CD25 was assessed before and after their stimulation with phorbol 12-myristate 13-acetate (PMA)/ionomycin, using flow cytometry (fluorescence-activated cell sorting; FACS) and confocal microscopy. Whole IVIg (Intraglobin F) was found to be able to inhibit the upregulation of CD25 expression, whereas this inhibitory effect was completely abolished in the IVIg-effluent compared with control (Figure 3). Specifically, IVIg (4 mg ml^{-1}) in the presence of PMA and ionomycin inhibited CD25 expression by ~43.3% (shifting mean fluorescence intensity from 103 to 58.6 ± 8.5), whereas the effluent (4 mg ml^{-1}) had no significant effect (mean fluorescence intensity = 104 ± 16.3; Figure 3a). This inhibitory effect could be observed at any concentration of ionomycin used (> 1 μg ml^{-1}), signifying a dominant effect of IVIg on CD25 induction (data not shown). Confocal microscopy analysis allowed for simultaneous visualization of CD25 expression and IVIg intracellular detection, showing that the non-penetrating fraction of IVIg (effluent) was unable to inhibit the upregulation of CD25 expression (Figure 3c). We further examined whether CD25 upregulation was affected on CD4$^+$ and/or CD8$^+$ activated splenocytes. Following the same procedure as above, it was shown that treatment with IVIg significantly inhibited the CD25 upregulation in CD4$^+$ splenocytes (control cells 22.1 ± 1.4%; IVIg 14.4 ± 0.9%, $P < 0.01$), whereas effluent did not present any alteration (control cells 22.1 ± 1.4%; effluent 20.7 ± 2.1%; Figure 3b). IVIg had no significant effect on CD25 upregulation in either CD8$^+$ (control cells 21.8 ± 2.1%; effluent 19.1 ± 1.9%; IVIg 15.7 ± 0.6%, $P = 0.065$) or CD8$^-$/CD4$^-$ splenocytes (control cells 56 ± 5.5%; effluent 67.1 ± 0.8%; IVIg 64.7 ± 3.2%; Figure 3b).

IVIg penetrates into cells from various organs after intravenous administration in mice

In vivo administration of disease-related monoclonal CPAbs into normal mice resulted in their penetration in cells of various organs.[4,28,29] To assess the ability of IVIg to penetrate into cells *in vivo*, two IVIg preparations were injected intravenously at 2 g kg^{-1} into BALB/c mice and 3 h later its distribution was detected in tissues from various organs. Confocal analysis showed intracellular presence of IVIg in the cells of almost all organs examined (Intraglobin F; Figure 4, Supplementary Figure 5 and Kiovig; Supplementary Figure 6). Specifically, liver cells presented high intracellular IVIg staining, which was increased in the vascular endothelium of liver blood vessels. Kidney glomeruli showed intense staining for IVIg, whereas lesser penetration was observed in the surrounding kidney cells. Lung and heart cells were evenly stained for intracellular IVIg, while ileum showed distinct strong staining of the lamina propria. In contrast to lamina propria, intestinal epithelia were poorly stained. Staining in the brain was solely localized in structures that correspond to microvessels as described previously when IVIg was directly injected in the brain circulation.[30] IVIg-organ distribution was also evaluated 6 days post administration of 2 g kg^{-1} of Intraglobin F-IVIg. Confocal analysis of lung, ileum and liver tissues revealed intracellular presence of IVIg (Figure 5). In detail, lung and ileum cells presented similar to the 3 h intracellular IVIg staining (all lung cells and ileum lamina propria were positive), but with lower fluorescent intensity. On the other hand, liver vascular endothelium showed intense IVIg staining, whereas liver parenchyma staining was markedly reduced (although, still over background). Analysis of cell suspensions obtained from spleen and lymph nodes showed that intracellular IVIg was localized essentially in the cytoplasm of the cells derived from spleen, whereas cells from lymph nodes were negative (Intraglobin F; Supplementary Figure 5A and Kiovig; Supplementary Figure 6B). The result was further verified by FACS analysis with mean values showing that spleen exhibited significant intracellular IVIg labeling (Intraglobin F; 48%, $P \leqslant 0.01$ Supplementary Figure 5B and Kiovig; 47%, $P \leqslant 0.01$ Supplementary Figure 6C). No significant fluorescence was detected in cells from all organs of control mice injected with physiological saline or effluent (IVIg depleted of CPAbs). Fluorescent labeling was specific for intracellular IVIg, as no significant fluorescence was detected when cells were analyzed without permeabilization (Supplementary Figure 5C). Thus, it seems like IVIg can readily access a wide range of tissues in which it penetrates a wide variety of cells, and primarily localizes to the cytoplasm.

DISCUSSION

Anti-nuclear autoantibodies in the sera of patients with systemic lupus erythematosus and mixed connective tissue disease that penetrate into living cells are well characterized,[2,5,29] known to exert different functions, such as induction of apoptosis, modulation of nuclear factor-kB and cytokine expression.[4–8] These disease-occurring CPAbs share common features, such as polyreactivity and germ-line gene encoding, with NAbs in normal human sera,[11,20,21] but it is intriguing that to date the physiologically occurring CPAbs have not been explored.

A common source of NAbs is IVIg preparation, a potent therapeutic product derived from sera of thousands of healthy donors. During our

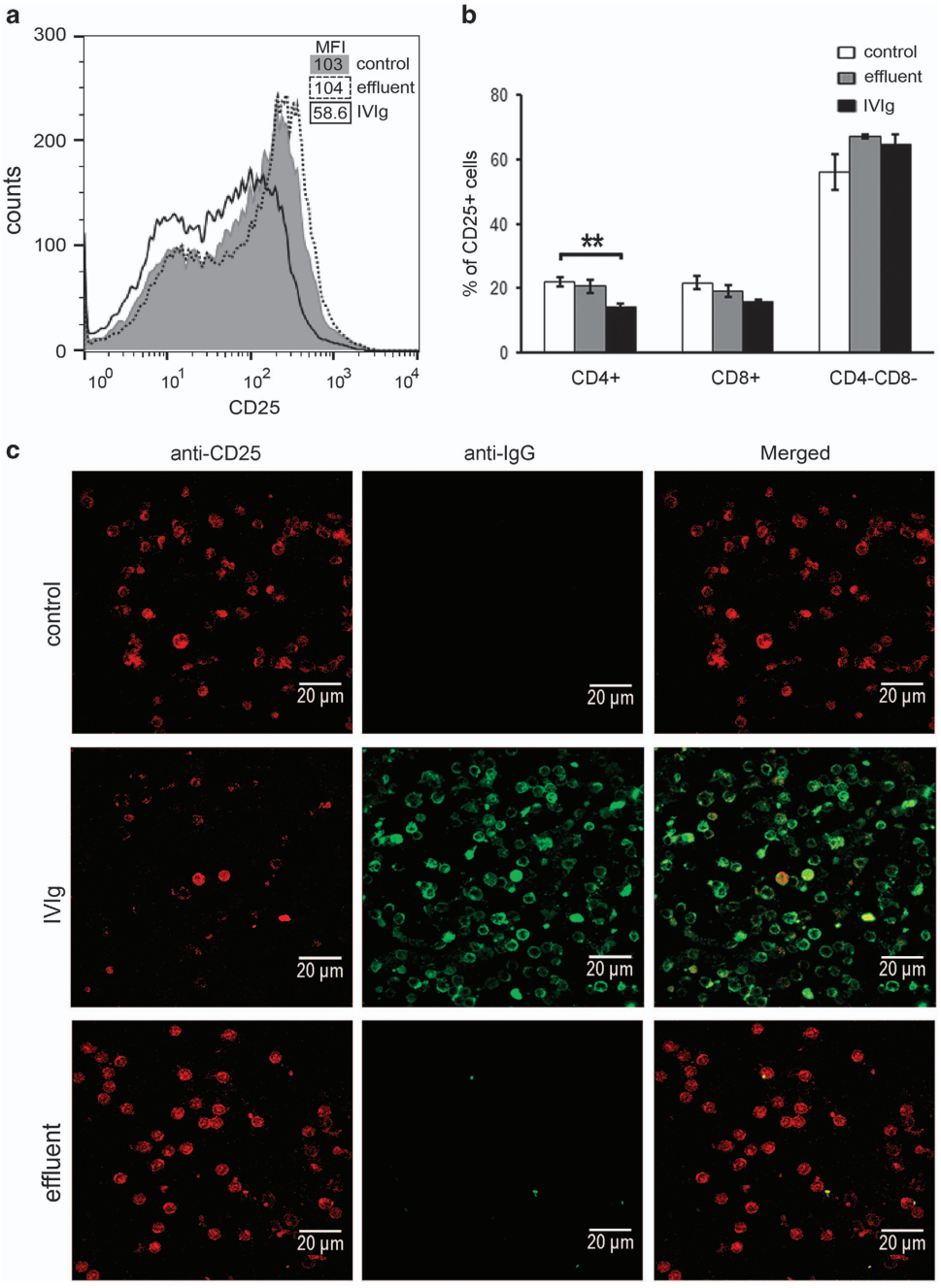

Figure 3 Effect of IVIg cell penetration on CD25-induced upregulation in $CD4^+$, $CD8^+$ and double negative splenocytes. Splenocytes from BALB/c mice were incubated for 90 min with 4 mg ml^{-1} of whole IVIg (Intraglobin F), 4 mg ml^{-1} of IVIg-effluent or culture medium (control) and then stimulated for 5 h with PMA (1 ng ml^{-1})/ionomycin (1 µg ml^{-1}) at 37 °C. (**a**) Fluorescent intensity of CD25 expression on stimulated splenocytes incubated with samples in the presence of PMA/ionomycin, and mean fluorescent intensity (MFI) of CD25 staining by FACS analysis ($n=7$). Results obtained from at least three independent experiments. (**b**) Percentages (%) of CD25-expressing cells in $CD4^+$, or $CD8^+$, and $CD4^-CD8^-$ populations. Results are shown as mean values of 4 (control) and 3 (effluent and IVIg) samples and are representative of three independent experiments. (**c**) Maximum projection of confocal sections of splenocytes. IVIg (green) and CD25 (red) observed using a x63 HCX PLApo objective lens; scale bar corresponds to 20 µm. Results are representative of three independent experiments.

extensive investigation, we found that IVIg could penetrate into a large series of cell types of mouse and human origin, which is consistent with previous studies on pathological CPAbs.[2,5,7] IVIg has been previously reported to internalize *in vitro*, into certain cell types, namely endothelial, dendritic and B cells.[22–24] Individual normal IgG, tested in parallel with IVIg, showed similar penetrating profile, strongly suggesting that CPAbs do occur under physiological conditions. This may exclude the possibility that this effect was due to the wide range of reactivities present in IVIg or to spurious antibody contamination from undiagnosed diseases. Individual sera possess probably variable contents of CPAbs, and the observed IVIg intracellular distribution is the result of pooled individual sera.

To better define the CPAbs present in IVIg, we purified three IgG fractions using IADs carrying antigens previously reported to be

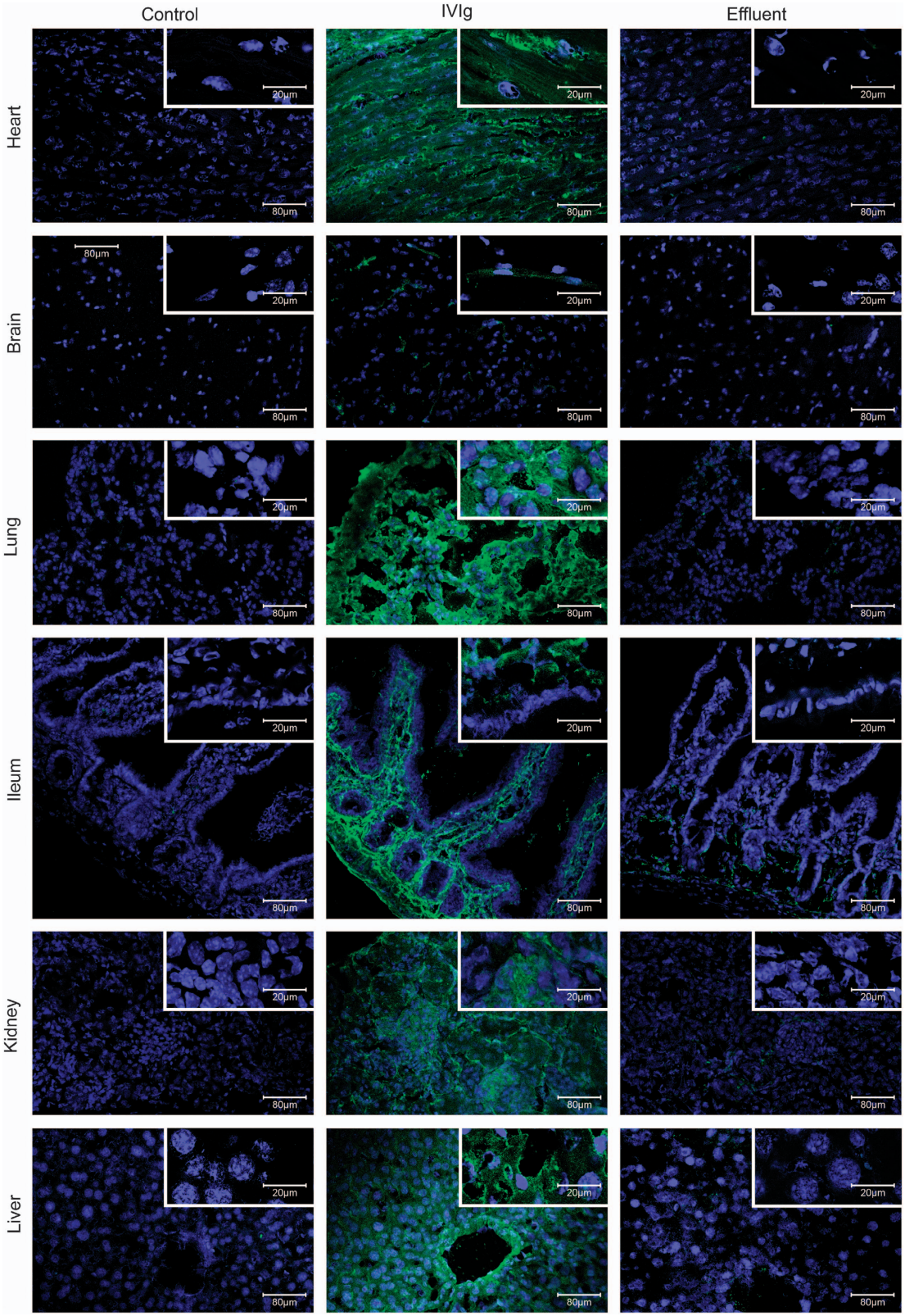

Figure 4 *In vivo* cell penetration of IVIg 3 h post administration. BALB/c mice received a single intravenous injection of 2 g kg^{-1} of IVIg (Intraglobin F; $n=3$), or IVIg-effluent ($n=3$), or physiological saline ($n=3$; control). Three hours later, various organs were snap-frozen and subjected to cryostat sectioning. Maximum projection of confocal sections from organs processed with cryostat (liver, kidneys, lungs, brain, ileum and heart). IVIg staining (green) and TO-PRO-3 iodide nucleus labeling (blue) observed using a x20 HC PlanApo and x63 HCX PLApo objective lenses; scale bar corresponds to either 80 or 20 μm. Results are representative of three independent experiments.

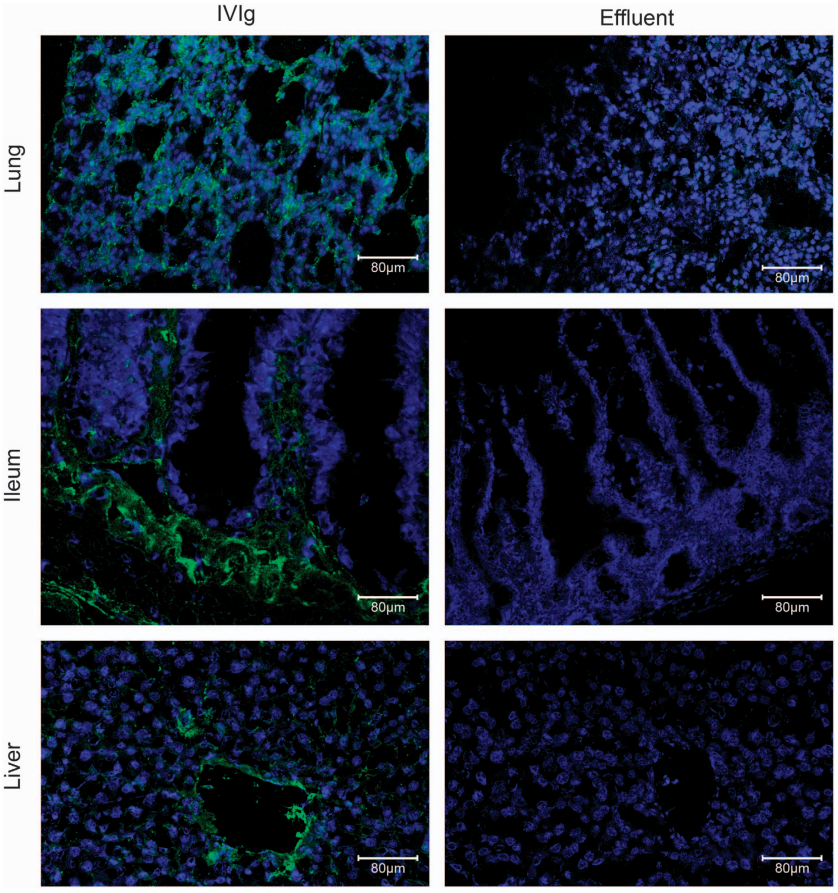

Figure 5 *In vivo* cell penetration of IVIg 6 days post administration. BALB/c mice received a single intravenous injection of 2 g kg^{-1} of IVIg (Intraglobin F; $n=3$) or of 2 g kg^{-1} of IVIg-effluent ($n=3$). Six days later, the lung, ileum and liver were snap-frozen and subjected to cryostat sectioning. Maximum projection of confocal sections from organs were processed with cryostat. IVIg staining (green) and TO-PRO-3 iodide nucleus labeling (blue) were observed using a x20 HC PlanApo objective lens; scale bar corresponds to 80 µm. Results are representative of three independent experiments.

associated with cell penetration: histone, heparin and DNA.[12–15] Unexpectedly, we found that the removal of these fractions, which corresponded to no more than 2% of IVIg, was crucial for the penetrating property of IVIg. This was accomplished by successive and exhaustive passages of IVIg on the three IADs. On the contrary, exhaustive passages on a single IAD removed up to 26–35.3% of the CPAbs and therefore it appears that heterogeneous fractions of CPAbs are present in IVIg. These affinity-purified fractions presented broad antibody reactivity to nucleic acids, proteins and haptens, property also exhibited by CPAbs derived from lupus-prone mice.[11] Specifically, the reactivity profile of histone-isolated fraction differed from that of heparin- and DNA-isolated ones, possibly due to the opposite charges of the target antigens (histone(+) vs heparin and DNA(−)). The similar profile shared by the latter two fractions is in line with previous studies showing high binding capacity of anti-DNA antibodies to heparin.[12]

Interestingly, naturally occurring CPAbs present in IVIg were found to accumulate in the cytoplasm, whereas CPAbs deriving from systemic lupus erythematosus and lupus-prone mice sera are described to localize in the nucleus, where they exert their function.[1,2,4–6,29] Despite this difference, these entities share polyreactivity to both nuclear and cytoplasmic constituents, a key property of the cell penetration process.[11] Indeed, affinity-purified IVIg-IgG fractions, even when purified against nuclear antigens, also reacted with cytoplasmic antigens. Subtle structural differences within the multi-binding site between natural- and pathological CPAbs might exist on the basis of their distinct intracellular localization, as previously described for autoantibodies.[31,32] The cytoplasmic localization of naturally occurring CPAbs might be related to the immunoregulatory role of IVIg,[26,33,34] which is opposed to the nuclear accumulation of autoimmune CPAbs described in lupus pathogenesis.[4,8,35]

Although, it is documented that IVIg can be internalized by endothelial cells through ligand–FcR-mediated endocytosis,[22] it has been also reported that the spontaneous FcR-independent internalization of IVIg occurs in immune cells.[23,24] Our results are in agreement with the latter, showing IVIg penetration in an energy-independent manner into a variety of cell lines several of which are not expressing Fc receptors.[36–38] In addition, the IVIg penetration into mouse cells detected *in vitro* and *in vivo*, also points toward a receptor-independent mode of entry, as the Fc part of human Igs and the mouse FcR are not considered so cross-reactive.[39] Similar cytoplasmic staining intensity for both isolated $F(ab')_2$ fragments and intact IVIg indicated that cell penetration is mainly $F(ab')_2$-mediated, without excluding, however, the possibility that an Fc-mediated uptake is also involved.

In our effort to examine the effect of IVIg cell penetration on the cell function(s), we focused on *in vitro* lymphocyte activation, taking advantage of the previously reported IVIg modulatory effect on this process.[40–43] Stimulation, as assessed by CD25-activation marker induction, of splenocytes with PMA/ionomycin was significantly reduced in the presence of IVIg, whereas IVIg free of CPAbs had

no effect. Analysis of specific splenocyte populations revealed that $CD4^+$ cells upon IVIg treatment had reduced CD25 expression, in contrast to $CD8^+$ and double negative cell populations where no effect was noted. However, the intracellular presence of IVIg found in the vast majority of splenocytes, *in vitro* and *in vivo*, cannot exclude the possibility that other accessory immune cells are also affected. This was the case of a study where IVIg was found to be internalized by APCs, blocking the antigen presentation process and resulting in the antigen-specific $CD4^+$ activation and proliferation.[24] Alterations on *in vitro* cell activation and proliferation of immune cells have been also reported for disease-occurring CPAbs.[1,44–46] All the above strongly support the relationship between antibody cell penetration process and subsequent cellular function, the mechanistic implications of which need to be further investigated.

Previous studies on the tissue distribution of disease-related CPAbs, either polyclonal or monoclonal, revealed their deposition in various organs, such as the kidney, liver, heart, intestine and spleen, after administration in normal mice, or in skin biopsies from autoimmune patients.[1,2,4,5,11,28,29] To recapitulate the cell-penetrating effect of IVIg *in vivo* under physiological conditions, we administered IVIg intravenously in mice. Examination of all representative tissues 3 h post administration showed that IVIg was intracellularly localized in various organs and cell types, in contrast to IVIg depleted of CPAbs, which could not penetrate the cells in all cases. Lymph nodes presented no intracellular IVIg, possibly reflecting the multitude of factors influencing antibody biodistribution, such as blood flow through the organs. Vascular cells in the liver, brain and kidney were strongly positive for IVIg staining as expected because of the direct contact with blood circulation. On the other hand, no obvious penetration was observed in brain neuronal cells, in accordance with the observation that limited amounts of IVIg are able to cross the brain–blood barrier.[30] However, the intracellular localization of IVIg into N2a cells enhances the potential accessibility of IVIg to neuron cells when brain–blood barrier is collapsed or leaky, as in the case of brain disorders and respective experimental models. Staining for IVIg of the intestine showed dominant lamina propria localization with minimal penetration in the epithelial cells, in accordance to previous observations; although the authors did not focus on the subcellular localization of IVIg.[47] The global distribution of cell-penetrating IVIg across organs may account for the positive effects of its administration in a variety of conditions such as mesenteric ischemia-reperfusion injury of the intestine,[47] brain Aβ deposit formation,[48] experimental autoimmune diseases,[49] experimental thrombotic microangiopathy,[50] sepsis,[51] pulmonary fibrosis[52] and Kawasaki disease.[53] In addition, the intracellular presence of IVIg in the lung, ileum and liver 6 days after administration suggests that cell penetration should be taken into consideration during assessment of IVIg clinical effect as treatment cycles of IVIg, in humans and mouse disease models, include daily, weekly and monthly administration.[49,54]

In conclusion, it is the first time that CPAbs are identified and characterized in normal human serum, showing, both *in vitro* and *in vivo*, preferential cytoplasmic localization, in contrast to disease-related CPAbs; the intracellular role of these NAb subsets remains to be investigated. Furthermore, it is demonstrated that distinct antibody fractions representing up to 2% of the whole IgG in IVIg are responsible for cell penetration and that their intracellular presence may modulate cellular activities. The broad biodistribution of IVIg CPAbs may represent a novel mechanism that enables the homeostatic effect of naturally occurring antibodies in a variety of pathophysiological conditions, and enrichment of IVIg with CPAbs might enhance its protective use.

METHODS

Animals

Adult BALB/c mice were bred in the animal facility of the Hellenic Pasteur Institute, and treated according to the European guidelines.

Cell lines

Adherent cell lines used were as follows: human cervical cancer cells (HeLa), primary human fibroblasts from skin explants of healthy volunteers, mouse fibroblasts (NIH-3T3), mouse neuroblastoma cells (N2a), monkey kidney epithelial cells (Vero) and human hepatocellular carcinoma (HepG2) (HeLa, NIH-3T3, Vero are known not to express Fc receptors.)[36–38] Cells were detached with 0.5% trypsin-EDTA (Gibco, Scotland, UK).

IVIg preparations, their derivatives and human sera

Three commercial IVIg preparations (>95% IgG) studied were as follows: Sandoglobulin (Sandoz, Basel, Switzerland), Intraglobin F (Biotest Pharma-GmbH, Dreieich, Germany) and Kiovig (Baxter Healthcare-Corporation, Halle, Germany). These were extensively dialyzed against sterile physiological saline, to get the same microenvironment, and kept under sterile conditions at 4 °C. $F(ab')_2$ fragments of the three IVIg preparations were produced by pepsin digestion (Boehringer Mannheim, Mannheim, Germany), as previously described.[55] Undigested IgG or Fc-fragments were removed using a protein-G-Sepharose (Pharmacia-Biotech, Uppsala, Sweden) column, according to the manufacturer's protocol, and $F(ab')_2$ purity was checked by sodium dodecyl sulfate-polyacrylamide gel electrophoresis. IgG fractions from five sera of healthy donors were isolated, as above, on protein-G-Sepharose (healthy donor IgG), tested in comparison to IVIg cell penetration.

Antigens

Nine antigens served as targets of IVIg and purified antibodies. Calf-thymus whole histone (type IIA), native DNA (type I) and bovine erythrocyte carbonic anhydrase were purchased from Sigma (Seelze, Germany). Heparin sodium salt from porcine intestinal mucosa was purchased from Calbiochem (Darmstadt, Germany). Human actin, tubulin, thyroglobulin, and IgG $F(ab')_2$ fragments, and trinitrophenyl–bovine serum albumin conjugate were prepared as previously described.[56,57]

Isolation of IVIg antibody fractions by affinity-chromatography

Heparin–Sepharose CL-6B IAD (Pharmacia Biotech) and in-house histone and DNA IADs were used. The latter were prepared with glutaraldehyde-activated polyacrylamide-agarose beads (IBF Biotechnics, Villeneuve la Garenne, France) as previously described.[58,59] Intraglobin F-IVIg was either passed 3–4 times through the same IAD or successively through the three IADs. Briefly, Intraglobin F-IVIg (100 mg) diluted in loading buffer (25 mM Tris-buffered saline for histone or heparin IADs and Tris-buffered saline containing 2.5 mM EDTA (Sigma) for DNA IAD) was incubated with the coated beads for 2 h, at room temperature. The IAD was then washed with loading buffer at 4 °C, until optical density (OD) of the effluent at 280 nm was below 0.010 and antibodies were isolated with appropriate elution buffers: 5 M $MgCl_2$ in 0.05 M Tris, pH 7, for histone and heparin IADs;[60] and 20 mM carbonate-bicarbonate buffer containing 5% dimethyl sulfoxide, pH 10.5, for DNA IAD.[61] The order by which the IADs were used was random, and every sample was exhaustively passed through (3–4 times) until no OD was measured in the eluted fraction before loading to the next IAD. Eluates and effluents were concentrated on PM-30 membrane-filters (Millipore, Billerica, MA, USA), dialyzed against Tris-buffered saline, IgG concentration was determined by OD at 280 nm and stored in aliquots at −80 °C.

Cell penetration analysis by confocal microscopy

To assess the cell-penetrating capacity of IVIg, cell lines (15×10^3) in complete medium (CM; Dulbecco's modified Eagle's medium (Biochrom, Berlin, Germany) containing 10% heat-inactivated fetal bovine serum (FBS; Gibco, Glasgow, UK) were allowed to adhere to microscope coverslips (Glaswarenfabrik, Sondheim/Rhön, Germany) in 24-well culture plates (Corning, Tewksbury, MA, USA) for 2 days until 60% confluency was achieved. Cells

were then washed with CM and further incubated with the samples (three IVIg preparations, their F(ab′)$_2$ fragments, the Intraglobin F-IVIg affinity-purified antibody fractions and the IVIg-effluent) and the controls (healthy donors' IgG and culture medium) at different concentrations in CM (3.2–0.05 mg ml^{-1}) for 2 h at 37 °C. After washing with 0.01 M phosphate-buffered saline pH 7.4 (PBS) and fixing the cells with absolute ethanol (Sigma) for 10 min at –20 °C, cells were washed with PBS and blocked with PBS containing 1% bovine serum albumin (PBS–BSA). For the detection of human IgG from different preparations (IVIg, immune-purified IgG fractions or IgG isolated from individual sera), goat anti-human IgG (heavy (H)- and light (L)-chain-specific and species-adsorbed) conjugated to Alexa Fluor-488 (1 μg ml^{-1} in PBS–BSA; Invitrogen, Paisley, UK) was added for 1 h at room temperature. The IVIg-F(ab')$_2$ fragments were detected with goat anti-human IgG F(ab')$_2$ secondary antibody conjugated to fluorescein isothiocyanate, not reacting with the Fc portion of human IgG (Thermo Scientific, Vienna, Austria). Far-red fluorescent dye TO-PRO-3 iodide (1 μM in PBS–BSA; Invitrogen) was added for the labeling of cell nuclei (blue). Coverslips were subsequently mounted with Mowiol 4–88-Reagent (Calbiochem). Cell-fluorescence was observed with a Leica confocal TCS-SP microscope (Leica Microsystems, Germany), equipped with laser Argon: 457, 488, 514 nm and laser He/Neon: 543, 633 nm. The objective lenses used were ×20 HC PlanApo (0.7 numerical aperture) and ×63 HCX PLApo (1.32 numerical aperture). Cells were subjected to optical sectioning (10–20 sections), moving stepwise (0.5 nm) and Leica confocal software (Leica) was used for image acquisition.

To investigate the mode of entry of IVIg, NIH-3T3 cells were preincubated for 30 min at 4 °C, where energy-dependent pathways are blocked, or at 37 °C in the presence of cytochalasin D (1 μg ml^{-1}; Sigma), an endocytosis/macropinocytosis inhibitor inducing disruption in actin microfilaments. Pretreated cells were then incubated with Sandoglobulin-IVIg for 2 h at 4 °C or at 37 °C in the presence of cytochalasin D followed by the procedure described above.

Assessment of IVIg antibody reactivity by ELISA

Polystyrene microtiter plates (Nunc, Roskilde, Denmark) were coated (overnight at 4 °C) with histone (2.5 μg ml^{-1}), heparin sodium salt (2 μg ml^{-1}), carbonic anhydrase (5 μg ml^{-1}), actin or tubulin (5 μg ml^{-1}), thyroglobulin (10 μg ml^{-1}), F(ab′)$_2$ fragments (1 μg ml^{-1}) or trinitrophenyl–bovine serum albumin (10 μg ml^{-1}) in 0.1 M carbonate-bicarbonate buffer, pH 9.6, whereas native DNA (10 μg ml^{-1}) was coated in PBS, pH 6.8. The antigen-coated plates were washed with PBS, blocked with PBS–BSA, and then incubated with the samples (the three IVIg, Intraglobin F-IVIg affinity-purified antibody fractions and respective effluents; 150–1.17 μg ml^{-1}) for 2 h at 37 °C. The wells were washed with PBS containing 0.1% Tween-20 (Merck, Darmstadt, Germany; PBS–T), and sheep anti-human IgG (H- and L-chain-specific) conjugated to horseradish peroxidase (0.8 μg ml^{-1} in PBS–T–BSA; Serotec, Oxford, UK) was added and incubated for 90 min at 37 °C. In human IgG F(ab′)$_2$-coated plates, goat anti-human IgG (γ-chain-specific) conjugated to alkaline phosphatase (0.5 μg ml^{-1} in PBS–T–BSA; Sigma) was used. The enzyme substrate, tetramethyl-benzidine (Seramun, Germany) or *p*-nitrophenyl-phosphate (Sigma), was added and OD was measured at 450 or 405 nm, respectively, with an ExpertPlus microplate reader (Asys, Eugendorf, Austria).

Cellular extracts preparation and quantification of intracellular IVIg

HeLa cells and human fibroblasts (9×10^4) were seeded onto six-well culture plates (Nunc) in CM (12 wells per sample), and incubated with the three IVIg (1.6 mg ml^{-1}) as performed in cell penetration assay. After washing with PBS, cells were detached with 0.5% trypsin-EDTA, counted and examined for viability with trypan blue (Sigma). Cytoplasmic and nuclear extracts were prepared after incubation with hypotonic lysis buffer, as previously described.[62] Protease inhibitors (7× complete mini, EDTA-free; Roche, Berlin, Germany) and 0.5 mM *dl*-dithiothreitol (Fluka, Seelze, Germany) were added to all buffers before use. IVIg in all extracts was quantified by ELISA. For this purpose, microtiter plates were coated with goat anti-human IgG (γ-chain-specific; 2 μg ml^{-1} in PBS; Sigma), and, after washing and blocking as above, these were incubated with extracts in serial threefold dilutions (1/3–1/81, in PBS–T–BSA) in duplicate wells. Serial dilutions of commercial human IgG, purified from pooled normal sera (125–0.97 ng ml^{-1}; Sigma) were used to obtain the standard semi log curve (with linear part: 31.25–7.81 ng ml^{-1} and IgG detection limit: 7.81 ng ml^{-1}). After washing, goat anti-human IgG (γ-chain-specific) conjugated to alkaline phosphatase (1 μg ml^{-1} in PBS–T–BSA; Sigma) was added and the procedure was completed as described above.

In vivo administration of IVIg

Adult BALB/c mice were intravenously injected with 2 g kg^{-1} of Intraglobin F-IVIg or controls (physiological saline or 2 g kg^{-1} of the effluent of Intraglobin F-IVIg), and killed 3 h or 6 days later. The same procedure was followed with Kiovig-IVIg (physiological saline as control) and the mice were killed 3 h later. The kidneys, liver, lungs, heart, ileum and brain were also removed, after perfusion with saline and subsequently analyzed immunohistochemically. Lymph nodes and spleens were prepared as single-cell suspensions using cell-dissociation sieves (Sigma). Cell suspensions were washed with RPMI (Gibco), treated with ammonium chloride–potassium buffer to lyse red blood cells and then trypsinized for 15 min at 37 °C. Cells were then washed with PBS, examined for viability and subsequently either fixed with absolute ethanol for 10 min at –20 °C or air-dried on coverslips and fixed, and then analyzed by FACS and confocal microscopy (as above), respectively.

For immunohistochemical analysis, tissues were snap-frozen in optimal cutting temperature compound (OCT; BDH, Vienna, Austria) and 10-μm-thick tissue sections were obtained with Leica CM-1900 cryostat onto superfrost slides (VWR international, Vienna, Austria). Cryostat sections were fixed in acetone for 10 min and processed for confocal microscopy analysis (see above).

For FACS analysis, after washing with PBS–BSA, the cells were incubated with goat anti-human IgG conjugated to Alexa Fluor-488 (1 μg ml^{-1} in PBS–BSA) for 40 min on ice. Finally, washed cells were analyzed with FACS Calibur (Becton Dickinson, Franklin Lakes, NJ, USA), equipped with an Argon laser. The CellQuest-Pro software program (Becton Dickinson) was used for data acquisition and analysis. To examine possible cell-surface binding of IVIg, cells were treated with 2% paraformaldehyde, permeabilized or not with 0.1% Triton X-100 in PBS-PSA, washed with PBS–BSA and then incubated with goat anti-human IgG conjugated to Alexa Fluor-488.

Splenocyte activation assay

Spleens from adult BALB/c mice were removed and homogenized separately with cell-dissociation sieves. Cell suspensions were washed with RPMI, treated with ammonium chloride–potassium buffer and assessed for cell viability. Cells (5×10^6 cells per well) were then cultured in six-well plates with RPMI containing 10% FBS (control), in the presence of Intraglobin F-IVIg (4 mg ml^{-1}) or its effluent (4 mg ml^{-1})—obtained after successive passages through the three IADs—for 90 min, at 37 °C. Half of the cells remained unstimulated (resting cells) and half were next stimulated with PMA (10 ng ml^{-1}; Sigma) plus ionomycin (1 μg ml^{-1}; Sigma) for 5 h, and washed with PBS–BSA. After activation, fixation with 2% paraformaldehyde was performed for 20 min at 4 °C, followed by washes with PBS. Cells were then incubated for 40 min on ice with anti-CD4-fluorescein isothiocyanate, anti-CD8-phycoerythrin or anti-CD25-allophycocyanin (BioLegend, San Diego, CA, USA 1 μg ml^{-1} in 3% FBS in PBS). Cells were then washed with PBS and analyzed by FACS. Mean fluorescence intensity and percentage of positive cells were determined by CellQuest-Pro software. To examine the penetration of Intraglobin F-IVIg, a portion of cells was also air-dried on coverslips, fixed with ethanol, incubated with goat anti-human IgG conjugated to Alexa Fluor-488 and anti-mouse CD25-phycoerythrin, and observed with the confocal microscope (see above).

Statistical analyses

These analyses were performed with either Student's two-tailed *t*-test or one-way analysis of variance and $P\leqslant0.05$ was considered significant.

CONFLICT OF INTEREST

The authors declare no conflict of interest.

ACKNOWLEDGEMENTS

We thank Mrs E Angelopoulos for the invaluable financial support and Dr P Papazafiri for kindly providing the primary human skin fibroblasts. AD Sali was supported by a scholarship for post-graduate studies from the State Scholarships Foundation. This work was partially supported by a grant from the Greek General Secretary of Research and Technology (ARISTEIA).

1 Alarcon-Segovia D, Ruiz-Arguelles A, Fishbein E. Antibody Penetration into Living Cells.1. Intranuclear immunoglobulin in peripheral-blood mononuclear-cells in mixed connective-tissue disease and systemic lupus-erythematosus. *Clin Exp Immunol* 1979; **35**: 364–375.
2 Golan TD, Gharavi AE, Elkon KB. Penetration of autoantibodies into living epithelial cells. *J Invest Dermatol* 1993; **100**: 316–322.
3 Yung S, Cheung KF, Zhang Q, Chan TM. Anti-dsDNA antibodies bind to mesangial annexin II in lupus nephritis. *J Am Soc Nephrol* 2010; **21**: 1912–1927.
4 Vlahakos D, Foster MH, Ucci AA, Barrett KJ, Datta SK, Madaio MP. Murine monoclonal anti-DNA antibodies penetrate cells, bind to nuclei, and induce glomerular proliferation and proteinuria *in vivo*. *J Am Soc Nephrol* 1992; **2**: 1345–1354.
5 Ruiz-Arguelles A, Alarcon-Segovia D. Penetration of autoantibodies into living cells, 2000. *Isr Med Assoc J* 2001; **3**: 121–126.
6 Madaio MP, Yanase K. Cellular penetration and nuclear localization of anti-DNA antibodies: mechanisms, consequences, implications and applications. *J Autoimmun* 1998; **11**: 535–538.
7 Ruiz-Arguelles A, Rivadeneyra-Espinoza L, Alarcon-Segovia D. Antibody penetration into living cells: Pathogenic, preventive and immuno-therapeutic implications. *Curr Pharm Design* 2003; **9**: 1881–1887.
8 Jang EJ, Nahm DH, Jang YJ. Mouse monoclonal autoantibodies penetrate mouse macrophage cells and stimulate NF-kappaB activation and TNF-alpha release. *Immunol Lett* 2009; **124**: 70–76.
9 Jang JY, Jeong JG, Jun HR, Lee SC, Kim JS, Kim YS *et al.* A nucleic acid-hydrolyzing antibody penetrates into cells via caveolae-mediated endocytosis, localizes in the cytosol and exhibits cytotoxicity. *Cell Mol Life Sci* 2009; **66**: 1985–1997.
10 Hansen JE, Chan G, Liu Y, Hegan DC, Dalal S, Dray E *et al.* Targeting cancer with a lupus autoantibody. *Sci Transl Med* 2012; **4**: 157ra142.
11 Ternynck T, Avrameas A, Ragimbeau J, Buttin G, Avrameas S. Immunochemical, structural and translocating properties of anti-DNA antibodies from (NZBxNZW) F1 mice. *J Autoimmun* 1998; **11**: 511–521.
12 Avrameas A, Gasmi L, Buttin G. DNA and heparin alter the internalization process of anti-DNA monoclonal antibodies according to patterns typical of both the charged molecule and the antibody. *J Autoimmun* 2001; **16**: 383–391.
13 Chan TM, Frampton G, Staines NA, Hobby P, Perry GJ, Cameron JS. different mechanisms by which Anti-DNA Moabs bind to human endothelial-cells and glomerular mesangial cells. *Clin Exp Immunol* 1992; **88**: 68–74.
14 Koutouzov S, Cabrespines A, Amoura Z, Chabre H, Lotton C, Bach JF. Binding of nucleosomes to a cell surface receptor: redistribution and endocytosis in the presence of lupus antibodies. *Eur J Immunol* 1996; **26**: 472–486.
15 Rakowicz-Szulczynska EM, McIntosh DG, Lewis P, Smith ML. Inhibition of cancer cell growth by internalized immuno-histone conjugates. *Cancer Biother Radiopharm* 1996; **11**: 77–86.
16 Yanase K, Smith RM, Puccetti A, Jarett L, Madaio MP. Receptor-mediated cellular entry of nuclear localizing anti-DNA antibodies via myosin 1. *J Clin Invest* 1997; **100**: 25–31.
17 Seddiki N, Nato F, Lafaye P, Amoura Z, Piette JC, Mazie JC. Calreticulin, a potential cell surface receptor involved in cell penetration of anti-DNA antibodies. *J Immunol* 2001; **166**: 6423–6429.
18 Zack DJ, Stempniak M, Wong AL, Taylor C, Weisbart RH. Mechanisms of cellular penetration and nuclear localization of an anti-double strand DNA autoantibody. *J Immunol* 1996; **157**: 2082–2088.
19 Alarcon-Segovia D, Ruiz-Arguelles A, Llorente L. Broken dogma: penetration of autoantibodies into living cells. *Immunol Today* 1996; **17**: 163–164.
20 Avrameas S, Ternynck T, Tsonis IA, Lymberi P. Naturally occurring B-cell autoreactivity: a critical overview. *J Autoimmun* 2007; **29**: 213–218.
21 Harindranath N, Ikematsu H, Notkins AL, Casali P. Structure of the VH and VL segments of polyreactive and monoreactive human natural antibodies to HIV-1 and *Escherichia coli* beta-galactosidase. *Int Immunol* 1993; **5**: 1523–1533.
22 Ronda N, Gatti R, Orlandini G, Borghetti A. Binding and internalization of human IgG by living cultured endothelial cells. *Clin Exp Immunol* 1997; **109**: 211–216.
23 Proulx DP, Aubin E, Lemieux R, Bazin R. Spontaneous internalization of IVIg in activated B cells. *Immunol Lett* 2009; **124**: 18–26.
24 Aubin E, Proulx DP, Trepanier P, Lemieux R, Bazin R. Prevention of T cell activation by interference of internalized intravenous immunoglobulin (IVIg) with MHC II-dependent native antigen presentation. *Clin Immunol* 2011; **141**: 273–283.
25 Ronda N, Leonardi S, Orlandini G, Gatti R, Bellosta S, Bernini F *et al.* Natural anti-endothelial cell antibodies (AECA). *J Autoimmun* 1999; **13**: 121–127.
26 Schwartz-Albiez R, Monteiro RC, Rodriguez M, Binder CJ, Shoenfeld Y. Natural antibodies, intravenous immunoglobulin and their role in autoimmunity, cancer and inflammation. *Clin Exp Immunol* 2009; **158**: 43–50.
27 Kaveri SV. Intravenous immunoglobulin: exploiting the potential of natural antibodies. *Autoimmun Rev* 2012; **11**: 792–794.
28 Abedi-Valugerdi M, Hu H, Moller G. Mercury-induced anti-nucleolar autoantibodies can transgress the membrane of living cells in vivo and in vitro. *Int Immunol* 1999; **11**: 605–615.
29 Alarcon-Segovia D. Antinuclear antibodies: to penetrate or not to penetrate, that was the question. *Lupus* 2001; **10**: 315–318.
30 St-Amour I, Pare I, Alata W, Coulombe K, Ringuette-Goulet C, Drouin-Ouellet J *et al.* Brain bioavailability of human intravenous immunoglobulin and its transport through the murine blood-brain barrier. *J Cerebr Blood Flow Met* 2013; **33**: 1983–1992.
31 Tsonis IA, Avrameas S, Moutsopoulos HM. Autoimmunity and pathophysiology. *J Autoimmun* 2007; **29**: 203–205.
32 Johnson PM, Watkins J, Scopes PM, Tracey BM. Differences in serum IgG structure in health and rheumatoid disease. Circular dichroism studies. *Ann Rheum Dis* 1974; **33**: 366–370.
33 Bayry J, Lacroix-Desmazes S, Carbonneil C, Misra N, Donkova V, Pashov A *et al.* Inhibition of maturation and function of dendritic cells by intravenous immunoglobulin. *Blood* 2003; **101**: 758–765.
34 Jacobi C, Claus M, Wildemann B, Wingert S, Korporal M, Romisch J *et al.* Exposure of NK cells to intravenous immunoglobulin induces IFN gamma release and degranulation but inhibits their cytotoxic activity. *Clin Immunol* 2009; **133**: 393–401.
35 AlarconSegovia D, Llorente L, RuizArguelles A. The penetration of autoantibodies into cells may induce tolerance to self by apoptosis of autoreactive lymphocytes and cause autoimmune disease by dysregulation and/or cell damage. *J Autoimmun* 1996; **9**: 295–300.
36 Castriconi R, Dondero A, Cantoni C, Della Chiesa M, Prato C, Nanni M *et al.* Functional characterization of natural killer cells in type I leukocyte adhesion deficiency. *Blood* 2007; **109**: 4873–4881.
37 Boonnak K, Slike BM, Donofrio GC, Marovich MA. Human FcgammaRII cytoplasmic domains differentially influence antibody-mediated dengue virus infection. *J Immunol* 2013; **190**: 5659–5665.
38 Rodrigo WW, Alcena DC, Kou Z, Kochel TJ, Porter KR, Comach G *et al.* Difference between the abilities of human Fcgamma receptor-expressing CV-1 cells to neutralize American and Asian genotypes of dengue virus 2. *Clin Vaccine Immunol* 2009; **16**: 285–287.
39 Bruhns P. Properties of mouse and human IgG receptors and their contribution to disease models. *Blood* 2012; **119**: 5640–5649.
40 MacMillan HF, Lee T, Issekutz AC. Intravenous immunoglobulin G-mediated inhibition of T-cell proliferation reflects an endogenous mechanism by which IgG modulates T-cell activation. *Clin Immunol* 2009; **132**: 222–233.
41 Klaesson S, Ringden O, Markling L, Remberger M, Lundkvist I. Immune modulatory effects of immunoglobulins on cell-mediated immune responses in vitro. *Scand J Immunol* 1993; **38**: 477–484.
42 Tawfik DS, Cowan KR, Walsh AM, Hamilton WS, Goldman FD. Exogenous immunoglobulin downregulates T-cell receptor signaling and cytokine production. *Pediatr Allergy Immunol* 2012; **23**: 88–95.
43 Trepanier P, Bazin R. Intravenous immunoglobulin (IVIg) inhibits CD8 cytotoxic T-cell activation. *Blood* 2012; **120**: 2769–2770.
44 Portales-Perez D, Alarcon-Segovia D, Llorente L, Ruiz-Arguelles A, Abud-Mendoza C, Baranda L *et al.* Penetrating anti-DNA monoclonal antibodies induce activation of human peripheral blood mononuclear cells. *J Autoimmun* 1998; **11**: 563–571.
45 Ma J, Chapman GV, Chen SL, Melick G, Penny R, Breit SN. Antibody penetration of viable human cells. I. Increased penetration of human lymphocytes by anti-RNP IgG. *Clin Exp Immunol* 1991; **84**: 83–91.
46 Nikolova KA, Tchorbanov AI, Djoumerska-Alexieva IK, Nikolova M, Vassilev TL. Intravenous immunoglobulin up-regulates the expression of the inhibitory FcgammaIIB receptor on B cells. *Immunol Cell Biol* 2009; **87**: 529–533.
47 Anderson J, Fleming SD, Rehrig S, Tsokos GC, Basta M, Shea-Donohue T. Intravenous immunoglobulin attenuates mesenteric ischemia-reperfusion injury. *Clin Immunol* 2005; **114**: 137–146.
48 Magga J, Puli L, Pihlaja R, Kanninen K, Neulamaa S, Malm T *et al.* Human intravenous immunoglobulin provides protection against Abeta toxicity by multiple mechanisms in a mouse model of Alzheimer's disease. *J Neuroinflammation* 2010; **7**: 90.
49 Ravindranath MH, Terasaki PI, Pham T, Jucaud V, Kawakita S. Therapeutic preparations of IVIg contain naturally occurring anti-HLA-E antibodies that react with HLA-Ia (HLA-A/-B/-Cw) alleles. *Blood* 2013; **121**: 2013–2028.
50 Jefferson JA, Suga SI, Kim YG, Pippin J, Gordon KL, Johnson RJ *et al.* Intravenous immunoglobulin protects against experimental thrombotic microangiopathy. *Kidney Int* 2001; **60**: 1018–1025.
51 McCuskey RS, Nishida J, McDonnell D, Baker GL, Urbaschek R, Urbaschek B. Effect of immunoglobulin G on the hepatic microvascular inflammatory response during sepsis. *Shock* 1996; **5**: 28–33.
52 Molina V, Haj-Yahia S, Solodeev I, Levy Y, Blank M, Shoenfeld Y. Immunomodulation of experimental pulmonary fibrosis by intravenous immunoglobulin (IVIG). *Autoimmunity* 2006; **39**: 711–717.
53 Yin JiX, Kang MR, Choi JS, Jeon HS, Han HS, Kim JY *et al.* Levels of intra- and extracellular heat shock protein 60 in Kawasaki disease patients treated with intravenous immunoglobulin. *Clin Immunol* 2007; **124**: 304–310.
54 Hartung HP, Mouthon L, Ahmed R, Jordan S, Laupland KB, Jolles S. Clinical applications of intravenous immunoglobulins (IVIg)–beyond immunodeficiencies and neurology. *Clin Exp Immunol* 2009; **158** (Suppl 1): 23–33.

55 Jones RG, Landon J. Enhanced pepsin digestion: a novel process for purifying antibody F(ab')(2) fragments in high yield from serum. *J Immunol Methods* 2002; **263**: 57–74.
56 Dighiero G, Lymberi P, Holmberg D, Lundquist I, Coutinho A, Avrameas S. High frequency of natural autoantibodies in normal newborn mice. *J Immunol* 1985; **134**: 765–771.
57 Cheng HF, Peterson RE, Evans TC. Preparation of highly purified human thyroglobulin. *Biochim Biophys Acta* 1968; **168**: 161–164.
58 Ternynck T, Avrameas S. Polyacrylamide-protein immunoadsorbents prepared with glutaraldehyde. *FEBS Lett* 1972; **23**: 24–28.
59 Ternynck T, Weston P, Guilbert B, Avrameas S. [A new process for the preparation of insoluble proteins and of proteins coupled with peroxidase]. *Ann Inst Pasteur (Paris)* 1972; **123**: 146–147.
60 Avrameas S, Ternynck T. The cross-linking of proteins with glutaraldehyde and its use for the preparation of immunoadsorbents. *Immunochemistry* 1969; **6**: 53–66.
61 Kubota T, Akatsuka T, Kanai Y. DNA affinity column chromatography: application in the isolation of distinct antibody populations from SLE sera. *Clin Exp Immunol* 1985; **62**: 321–328.
62 Timchenko N, Wilson DR, Taylor LR, Abdelsayed S, Wilde M, Sawadogo M *et al*. Autoregulation of the human C/EBP alpha gene by stimulation of upstream stimulatory factor binding. *Mol Cell Biol* 1995; **15**: 1192–1202.

The Supplementary Information that accompanies this paper is available on the Clinical and Translational Immunology website (http://www.nature.com/cti)